RSC Advances

PAPER

View Article Online
View Journal | View Issue

Cite this: *RSC Adv.*, 2018, **8**, 34560

Adsorption and visible-light photodegradation of organic dyes with TiO_2/conjugated microporous polymer composites†

Jisi Li, Xianhui Wen, Qiujing Zhang and Shijie Ren *

Received 1st August 2018
Accepted 2nd October 2018

DOI: 10.1039/c8ra06491a

rsc.li/rsc-advances

A series of composite materials made of TiO_2 and conjugated microporous polymers (CMPs) were prepared with a hydrothermal method and used as both adsorbents and photocatalysts for the adsorption and visible-light photodegradation of organic dyes in aqueous solutions. It is found that the blending of CMPs can significantly improve both the adsorption capacity and the photocatalytic degradation activity of TiO_2 towards organic dyes.

Introduction

Rapid industrialization and ever-growing human activities have caused more and more serious water pollution in the last few decades, posing great threats towards both human health and ecological environment. Organic dyes, as one of the major water pollutants, are usually toxic, chemically stable and hard to degrade.[1,2] Among various water treatment technologies, physisorption has been considered to be one of the most economic and effective methods to remove organic dyes in aqueous solutions.[3–6] However, traditional porous materials can only adsorb organic dyes without degradation, often suffering from regeneration and secondary pollution problems.[7] At present, photocatalysis is widely used in environmental remediation,[8,9] and photodegradation has been under active investigation as one of the effective emerging technologies for the elimination of organic dyes from water.[10] At present, most studies are focused on inorganic semiconductors as photocatalysts to degrade organic dyes, such as TiO_2 (ref. 11 and 12) and other metal oxides and sulphides.[13–16] However, these inorganic semiconductors often suffer from limited surface area and wide band gap (only UV responsive), severely restricting their practical applications.[17–19] Hence, it is highly desirable to develop material systems which can simultaneously adsorb organic dyes in aqueous solutions and photodegrade them under visible light.

With the above requirements in mind, conjugated microporous polymers (CMPs) which were firstly developed in 2007,[20] might be a new option. The distinguished properties of CMPs which include high stability and hydrophobicity, large surface area, full conjugation and high photon-activity endow them ideal candidates for the adsorption and photodegradation of organic dyes in aqueous solution.[21,22] Although CMPs have been extensively studied as photocatalysts for organic reactions or hydrogen evolution by water splitting,[23,24] there are few reports of CMPs as photocatalysts for degradation of organic pollutants.[25,26] Meanwhile, it has been well evidenced in organic photovoltaics that fabrication of heterojunction structure with organic–inorganic semiconductor composites is an efficient way to improve photogenerated charge separation,[27,28] which would also be highly beneficial for photodegradation.[29]

Herein, we prepared a triazine-containing CMP (TrCMP) *via* Suzuki coupling reaction. TrCMP shows reasonable adsorption capacity and high photodegradation activity towards a typical organic dye of methylene blue (MB) in aqueous solution. Then, TrCMP–TiO_2 composites with different TrCMP proportions were prepared with hydrothermal method. These composite materials exhibit variable adsorption capacities and photodegradation activities according to the content of TrCMP and with optimized feeding ratios, the composite materials show several times higher photodegradation rate than pure TiO_2 used separately.

Experimental

Chemicals

4-Bromobenzonitrile (98%+, Adamas), methylene blue (J&K), trifluoromethanesulfonic acid (99%, Adamas), 1,4-bis(4,4,5,5-tetramethyl-1,3,2-dioxaborolan-2-yl)benzene (98%+, Adamas), tetrakis(triphenylphosphine)palladium ($Pd(PPh_3)_4$, 9.2% Pd, Adamas), anhydrous *N*,*N*-dimethylformamide (DMF, 99.9%, J&K), TiO_2 (P25, Acros), dry $CHCl_3$, K_2CO_3, triethanolamine (TEOA, 99%, Kelong), benzoquinone (BQ, 99%, Adamas), $NaHCO_3$, ethanol, methanol, acetone, chloroform, and tetrahydrofuran are all purchased from commercial sources and used as received. Monomer Tr-M (2,4,6-tris(4-bromophenyl)-

College of Polymer Science and Engineering, State Key Laboratory of Polymer Materials Engineering, Sichuan University, Chengdu, 610065, P. R. China. E-mail: rensj@scu.edu.cn

† Electronic supplementary information (ESI) available. See DOI: 10.1039/c8ra06491a

1,3,5-triazine) was synthesized by 4-bromobenzonitrile according to the reported procedure.[30]

Synthesis of TrCMP

Under an argon atmosphere, Tr-M (164 mg, 0.3 mmol), 1,4-bis(4,4,5,5-tetramethyl-1,3,2-dioxaborolan-2-yl)benzene (149 mg, 0.45 mmol) and K_2CO_3 (1.66 g, 12 mmol) were dissolved in a mixture of DMF (40 mL) and water (6 mL). After degassed by argon for 1 h, $Pd(PPh_3)_4$ (17.31 mg, 0.015 mmol) was added to the mixture and the mixture was degassed for another 0.5 h. Then the solution was heated to 150 °C and stirred for 96 h. After cooled to room temperature, the mixture was poured into water and filtered. The solid was thoroughly washed with methanol, chloroform, acetone and tetrahydrofuran. Further purification was carried out by Soxhlet extraction with methanol, chloroform, and tetrahydrofuran for 24 h each. The resulting gray power was dried under vacuum at 120 °C for 24 h to get TrCMP (123 mg, 98%). Elemental analysis calcd (%) for $C_{30}H_{18}N_3$: C 85.69, H 4.31, N 9.99, C/N 7.93; found (%): C 85.64, H 4.82, N 7.97, C/N 10.75. Fourier-transform infrared spectroscopy (FT-IR) (KBr, cm^{-1}): 2921, 1607, 1577, 1512, 1423, 1365, 807.

Synthesis of TrCMP–TiO_2 composites

TrCMP was ultrasonicated in the mixture of deionized water (60 mL) and anhydrous ethanol (30 mL) to be completely dispersed. Then, different amount of TiO_2 was added to the dispersion and stirred vigorously for 2 hours to obtain a homogeneous suspension. This suspension was then transferred to a Teflon-sealed autoclave (100 mL) and maintained at 120 °C for 24 h. The resulting complex was collected by filtration, washed with water, and dried at 80 °C in vacuum to get the final composites with different addition ratios of TrCMP.

3% TrCMP–TiO_2: TrCMP (4.5 mg), TiO_2 (145.5 mg) to get 3% TrCMP–TiO_2 (147.5 mg, $Y = 98.33\%$).
5% TrCMP–TiO_2: TrCMP (7.5 mg), TiO_2 (142.5 mg) to get 5% TrCMP–TiO_2 (146.6 mg, $Y = 97.67\%$).
10% TrCMP–TiO_2: TrCMP (15 mg), TiO_2 (135 mg) to get 10% TrCMP–TiO_2 (144.8 mg, $Y = 96.53\%$).
20% TrCMP–TiO_2: TrCMP (30 mg), TiO_2 (120 mg) to get 20% TrCMP–TiO_2 (147.7 mg, $Y = 98.46\%$).

Photodegradation performance of TrCMP

For the adsorption test of TrCMP towards MB, aqueous solution of the MB dyes (5.4×10^{-5} mol L^{-1}, 35 mL), TEOA (4 mL), and TrCMP (10 mg) were placed in a beaker, and the sample was named "MB". Then, the solution was stirred in the dark, and individual samples were collected at 30 min intervals. After the solid TrCMP was removed by centrifugation, concentrations of the residue MB solutions (named "0.5 h, 1 h and 1.5 h", respectively) were tested by UV-vis absorption measurement. In addition, the same method was used to study the photodegradation performance of TrCMP towards MB. Before irradiation, the suspension was stirred under dark for 1 hour to reach adsorption–desorption equilibrium (named "0 min"). Then, the beaker was exposed to the visible irradiation produced by a 300 W Xe lamp with a cut-off filter ($\lambda > 420$ nm). During the illumination, about 4 mL of aliquot was sampled at the interval of 10 min over 60 min, and the solid was removed by centrifugation. The concentrations of the residue MB solutions (named "10 min, 20 min, 30 min, 40 min, 50 min and 60 min", respectively) were tested by the UV-vis absorption measurement.

Photodegradation performance of TrCMP–TiO_2

The photodegradation test method of TrCMP–TiO_2 composites was similar to that of TrCMP. MB solution (2.7×10^{-5} mol L^{-1}, 35 mL), TEOA (4 mL) and photocatalysts (TiO_2, 3% TrCMP–TiO_2, 5% TrCMP–TiO_2, 10% TrCMP–TiO_2, 20% TrCMP–TiO_2, 26.25 mg) were used in the measurement.

Results and discussion

As shown in Scheme 1, the triazine-containing CMP (TrCMP) was synthesized by Suzuki–Miyaura polycondensation reaction. Then, TrCMP and TiO_2 with different feed ratios were mechanically mixed in dispersion solutions, followed by a hydrothermal process, giving rise to a series of robust TrCMP–TiO_2 composites. Both TrCMP and the composite materials are insoluble in all solvents tested including water, methanol, dichloromethane, toluene, tetrahydrofuran, chloroform, DMF.

As we can see from the FT-IR spectra of triazine monomer Tr-M and polymer TrCMP (Fig. S1a, see ESI†), both of them exhibit strong stretching vibration peaks of triazine ring at 1512 and 1423 cm^{-1}. For the TrCMP–TiO_2 composites (Fig. S1b†), the intensity of triazine stretching vibration peak gradually increases with the increment of the proportion of TrCMP, indicating that the success of hydrothermal reaction. Thermal stability of the materials was evaluated by thermogravimetric analysis under a nitrogen atmosphere as shown in Fig. S2.† It can be clearly observed that TrCMP starts to decompose at around 450 °C, while TiO_2 is fairly stable until 800 °C. The remaining weight percentages of the composite materials at 800 °C correspond well with their individual components, corroborating the formation of the composite materials.

Scanning electron microscopy (SEM) images of the above materials are shown in Fig. S3.† While TiO_2 exhibits a morphology of dispersed particles (Fig. S3a†), TrCMP shows rod-shaped morphology with spherical particles on the surface (Fig. S3b†). Compared with pure TrCMP, TrCMP–TiO_2

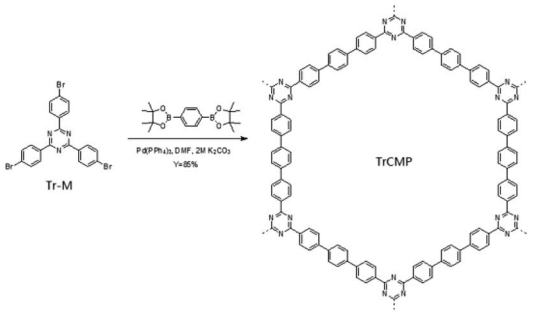

Scheme 1 The preparation route of TrCMP.

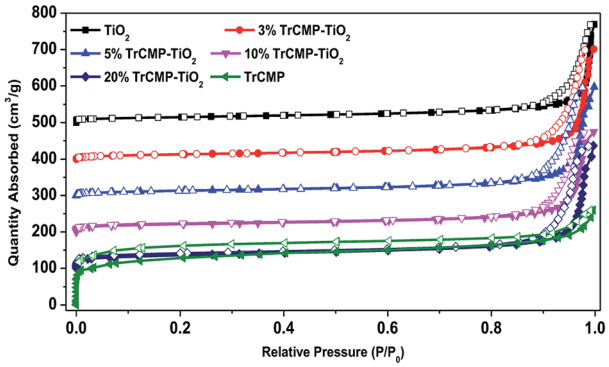

Fig. 1 Nitrogen adsorption/desorption isotherms of the materials at 77 K (the adsorption branch is labeled with filled symbols and desorption branch is labeled with open symbols). For clarity, the curves of 20% TrCMP–TiO_2, 10% TrCMP–TiO_2, 5% TrCMP–TiO_2, 3% TrCMP–TiO_2, and TiO_2 are shifted vertically by 100, 200, 300, 400, 500 cm^3 g^{-1}, respectively.

composite materials show much denser particles on the surface, indicating the successful complex of TiO_2 and TrCMP. High Resolution Transmission Electron Microscopy (HRTEM) images of 10% TrCMP–TiO_2 were measured as the example to investigate the interface between TiO_2 and the CMP. As shown in Fig. S4,† TrCMP is distributed on the TiO_2 surface and no obvious lattice fringe can be observed, revealing the tight contact between TiO_2 and TrCMP and the formation of heterojunction.

Porous properties of the materials were evaluated by nitrogen adsorption/desorption measurements at 77 K and the adsorption isotherms are shown in Fig. 1. TrCMP exhibits typical type I nitrogen sorption isotherms, indicating that there are a large number of micropores in the polymer. BET surface areas of TiO_2, 3% TrCMP–TiO_2, 5% TrCMP–TiO_2, 10% TrCMP–TiO_2, 20% TrCMP–TiO_2 and TrCMP are calculated to be 45, 49, 50, 75, 126 and 423 m^2 g^{-1}, respectively. Obviously, with the increase of TrCMP content, BET surface areas of the composite materials increase accordingly. UV-vis absorption spectra of the materials are shown in Fig. S5† and it is found that maximum absorption wavelengths of the composite materials gradually red-shift with the increase of TrCMP proportion, indicative of broader light absorption, especially in the visible light range.

As a photon-active conjugated polymer network with abundant porous structure, TrCMP is supposed to be an ideal candidate for adsorption and photodegradation of organic pollutant in aqueous solution. Herein, methylene blue (MB) was used as the model organic dye to test adsorption capacity and photocatalytic activity of TrCMP and the adsorption process was monitored by the absorbance variation of MB at 664 nm. Control experiment reveals that when the aqueous solution of MB without any photocatalyst was irradiated under visible light for 1 h, the self-photodegradation of MB was negligible. As shown in Fig. 2a, the absorption intensity of MB exhibits a significant decrease after stirred with TrCMP for 0.5 h, and the intensity has no obvious change when it comes to 1 h and 1.5 h, which means that it only needs 0.5 h for TrCMP to get the adsorption–desorption equilibrium. The adsorption amount

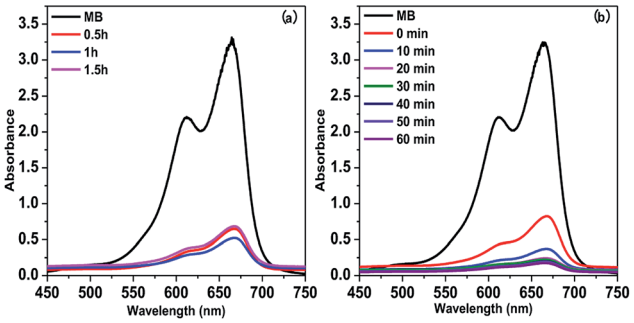

Fig. 2 (a) Time-dependent UV-vis absorption spectra of MB in aqueous solution with the presence of TrCMP under dark, (b) time-dependent UV-vis absorption spectra of MB in aqueous solution with the presence of TrCMP under visible light (λ > 420 nm) irradiation.

(Q) of TrCMP is calculated to be 50.87 mg g^{-1} at a very dilute solution of MB (5.4×10^{-5} mol L^{-1}), indicating TrCMP has good capacity for MB adsorption even at low concentration. Then, photocatalytic activity of TrCMP towards the degradation of MB was measured after the adsorption–desorption equilibrium was reached and the results are shown in Fig. 2b. Under the irradiation of visible light (λ > 420 nm), absorbance intensity of MB further decreases and it takes TrCMP only 20 minutes to degrade 92.5% of MB, demonstrating efficient photocatalytic activity of TrCMP under visible light.

Adsorption and photodegradation properties of the TrCMP–TiO_2 composites towards MB under visible light irradiation were also measured and the results are shown in Fig. 3. Pure TiO_2 shows moderate photodegradation towards MB and along the increase of TrCMP content, the composite materials exhibit much better photodegradation performances. According to the absorbance decay spectra of MB (Fig. 2b and 3a–e), adsorption and photodegradation kinetics curves of TiO_2, TrCMP and the composite materials are shown in Fig. 3f. As illustrated in Table 1, the adsorption amounts (Q) of TiO_2, 3% TrCMP–TiO_2, 5% TrCMP–TiO_2, 10% TrCMP–TiO_2, and 20% TrCMP–TiO_2 are calculated to be 2.83, 4.02, 4.21, 6.99 and 9.61 mg g^{-1} respectively, which are in direct proportion to the specific surface areas of the materials. Furthermore, it reveals that all of the photodegradation progresses approximately follow first-order dynamic models (Fig. 4). According to the slopes of the curves, photodegradation rates (K) of TiO_2, 3% TrCMP–TiO_2, 5% TrCMP–TiO_2, 10% TrCMP–TiO_2, 20% TrCMP–TiO_2 and TrCMP are calculated to be −0.0056, −0.0047, −0.0173, −0.0359, −0.0259 and 0.0219 min^{-1} respectively (Table 1). Interestingly, 10% TrCMP–TiO_2 shows the highest photocatalytic activity towards MB, much higher than either TiO_2 or TrCMP used separately.

As discussed in previous literatures,[29,31] superoxide radical ($\cdot O_2^-$) and photogenerated hole (h^+) are possible reactive species in photodegradation of dye molecules. To figure out the mechanism of MB degradation, a series of control experiments with different scavengers using 10% TrCMP–TiO_2 as the photocatalyst were conducted. Benzoquinone (BQ, the $\cdot O_2^-$ scavenger, 1×10^{-3} mol L^{-1}), and $NaHCO_3$ (the h^+ scavenger, 2×10^{-3} mol L^{-1}) were separately added to the photodegradation

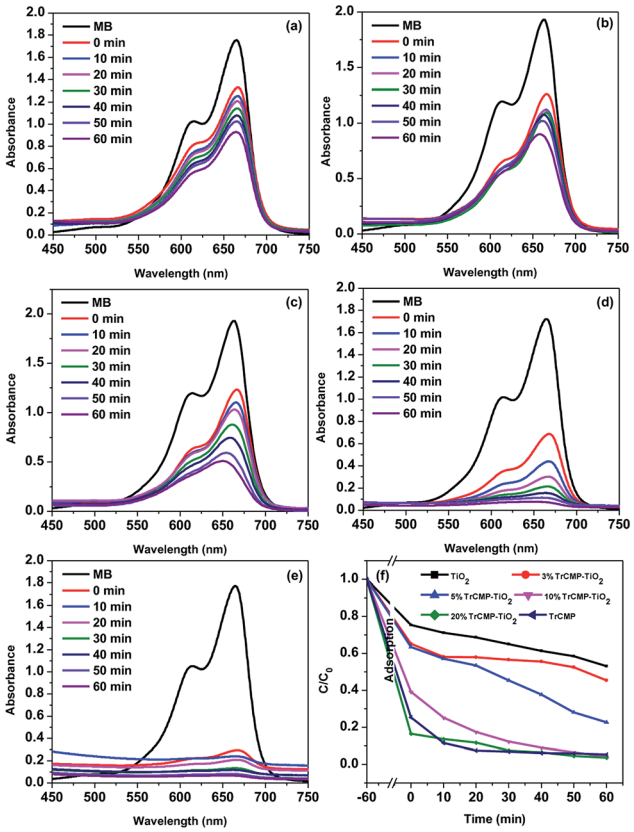

Fig. 3 Time-dependent UV-vis absorption spectra of MB in aqueous solution with the presence of (a) TiO_2; (b) 3% TrCMP–TiO_2; (c) 5% TrCMP–TiO_2; (d) 10% TrCMP–TiO_2 and (e) 20% TrCMP–TiO_2 under visible light (λ > 420 nm) irradiation; and (f) adsorption and photodegradation kinetics curves of various photocatalysts towards MB under visible light (λ > 420 nm) irradiation.

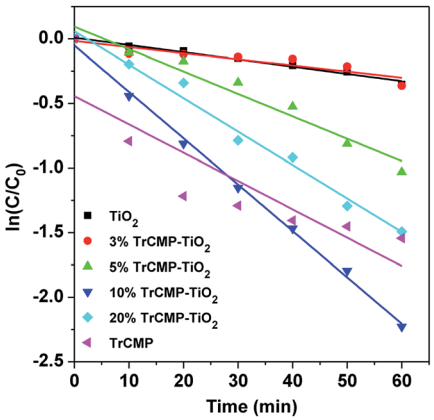

Fig. 4 Photodegradation reaction kinetics with visible light (λ > 420 nm) irradiation in presence of various photocatalysts.

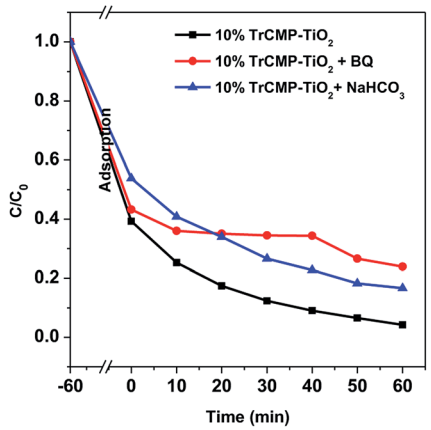

Fig. 5 Photodegradation kinetics of MB on 10% TrCMP–TiO_2 under visible light (λ > 420 nm) with different scavengers (1×10^{-3} mol L^{-1} benzoquinone and 2×10^{-3} mol L^{-1} $NaHCO_3$).

system to verify the reaction mechanism. As illustrated in Fig. 5, the absence of $\cdot O_2^-$ or h^+ both cause a significant activity decrease, indicating that $\cdot O_2^-$ and h^+ simultaneously participate in the degradation process of MB. In addition, the degradation of MB is more obviously depressed by the BQ, revealing that $\cdot O_2^-$ is likely to be the primary active species in the degradation process, which is consistent with previous reports.[26,32]

The introduction of TrCMP onto TiO_2 broadens its visible light absorption and more protons can be absorbed to form electron–hole pairs. The formed heterojunction between TrCMP and TiO_2 can accelerate the e^-/h^+ separation and inhibit the recombination of the photogenerated electron–hole pairs; as a result, more holes can play a role in the photodegradation of MB. Simultaneously, more photogenerated electrons can react with O_2 to form more $\cdot O_2^-$ radicals. To sum up, broadened light absorption, enhanced photogenerated charge separation and radical generation significantly improve the photodegradation performance of the composite materials. However, when the amount of TrCMP exceeds the optimal value, it might start to aggregate, resulting in the decrease of photodegradation rate.[33,34]

Table 1 Adsorption amount and photodegradation rate of various photocatalysts in the degradation of MB

Photocatalyst	S_{BET} (m^2 g^{-1})	Adsorption amount (Q) (mg g^{-1})	Photodegradation rate (K) (min^{-1})
TiO_2	45.1	2.83	−0.0056
3% TrCMP–TiO_2	48.5	4.02	−0.0047
5% TrCMP–TiO_2	50.0	4.21	−0.0173
10% TrCMP–TiO_2	74.7	6.99	−0.0359
20% TrCMP–TiO_2	125.5	9.61	−0.0259
TrCMP	423.0	50.87	−0.0219

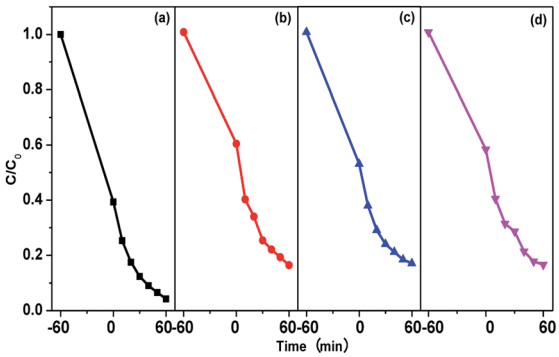

Fig. 6 Cycling runs for the photodegradation of MB with 10% TrCMP–TiO_2 (a) the first photodegradation test; (b) cycle 1; (c) cycle 2; and (d) cycle 3.

What should be mentioned is that the photodegradation not only happens to the MB molecules in the aqueous solution, but also the MB molecules that are confined in the pores of the photocatalysts. When the concentration of MB in aqueous solution decreases because of the degradation, the MB molecules confined by the pores will diffuse to the solution to be further photodegraded. To verify this, 10% TrCMP–TiO_2 was collected from the photodegradation system after irradiation for 60 min under visible light and redispersed in extra 4 mL of water. UV-vis absorption measurement of the dispersion eluent shows there is no residual MB left inside pores of 10% TrCMP–TiO_2 (Fig. S6†), illustrating excellent regeneration property of the photocatalyst. Additionally, cycling experiments were carried out to evaluate the stability and reusability of the TrCMP–TiO_2 composites. As shown in Fig. 6 and Table S1,† in the first run, 10% TrCMP–TiO_2 shows a photodegradation rate of 0.0359 min^{-1} and can remove 96% of MB in 60 min. After three cycle tests, 10% TrCMP–TiO_2 still exhibits a high photodegradation rate of 0.0317 min^{-1} and removal ratio of 92%. This shows that the composite material of 10% TrCMP–TiO_2 can be used as an efficient heterogeneous photocatalyst with excellent cycle performance to degrade MB in aqueous solution.

Conclusions

In summary, a triazine-containing CMP (TrCMP) was prepared *via* Suzuki coupling reaction. TrCMP shows reasonable adsorption capacity and high photocatalysis activity for the photodegradation of methylene blue (MB) in aqueous solution. TrCMP–TiO_2 composites with different TrCMP proportions were prepared with hydrothermal method. These composite materials exhibit variable photodegradation rate according to the content of TrCMP. Among them, 10% TrCMP–TiO_2 shows the highest photodegradation rate of 0.0359 min^{-1} and can remove 96% of MB in 60 min in a dilute aqueous solution under visible light irradiation. These values are comparable to some of the newly developed photocatalysts.[27,34] Meanwhile, the photocatalytic performance of 10% TrCMP–TiO_2 shows no obvious decrease after 3 cycle tests. The use of conjugated microporous polymers and their composite materials as both adsorbents and photocatalysts for the removal of organic dyes in water provides a valuable insight towards wastewater treatment.

Conflicts of interest

The authors confirm that there are no conflicts to declare.

Acknowledgements

This work is financially supported by National Natural Science Foundation of China (21574087, 21404074) and China Postdoctoral Science Foundation (2015M570785).

References

1 H. Zhang, X. Lv, Y. Li, Y. Wang and J. Li, *ACS Nano*, 2010, **4**, 380–386.
2 A. A. Adeyemo, I. O. Adeoye and O. S. Bello, *Toxicol. Environ. Chem.*, 2012, **94**, 1846–1863.
3 J. Yuan, X. Liu, O. Akbulut, J. Hu, S. L. Suib, J. Kong and F. Stellacci, *Nat. Nanotechnol.*, 2008, **3**, 332–336.
4 I. Ali, *Chem. Rev.*, 2012, **112**, 5073–5091.
5 P. Basnet and Y. P. Zhao, *J. Mater. Chem. A*, 2014, **2**, 911–914.
6 Z. Zhu, Y. L. Bai, L. Zhang, D. Sun, J. Fang and S. Zhu, *Chem. Commun.*, 2014, **50**, 14674–14677.
7 M. Chhabra, S. Mishra and T. R. Sreekrishnan, *Biochem. Eng. J.*, 2015, **93**, 17–24.
8 W. Cui, J. Y. Li, Y. J. Sun, H. Wang, G. M. Jiang, S. C. Lee and F. dong, *Appl. Catal., B*, 2018, **237**, 938–946.
9 H. Wang, Y. Sun, G. Jiang, Y. Zhang, H. Huang, Z. Wu, S. C. Lee and F. Dong, *Environ. Sci. Technol.*, 2018, **52**, 1479–1487.
10 J. Lu, J. X. Lin, X. L. Zhao and R. Cao, *Chem. Commun.*, 2012, **48**, 669–671.
11 A. Yousef, M. M. El-Halwany, N. A. M. Barakat, M. N. Al-Maghrabi and H. Y. Kim, *J. Ind. Eng. Chem.*, 2015, **26**, 251–258.
12 D. Loncarevic, J. Dostanic, V. Radonjic, L. Zivkovic and D. M. Jovanovic, *React. Kinet. Catal. Lett.*, 2016, **118**, 153–164.
13 G. T. S. T. da Silva, K. T. G. Carvalho, O. F. Lopes, E. S. Gomes, A. R. Malagutti, V. R. Mastelaro, C. Ribeiro and H. A. J. L. Mourão, *ChemCatChem*, 2017, **9**, 3795–3804.
14 C. C. Keong, Y. S. Vivek, B. Salamatinia and B. A. Horri, *J. Phys.: Conf. Ser.*, 2017, **829**, 012014.
15 I. F. Ertis and I. Boz, *Int. J. Chem. React. Eng.*, 2017, **15**, 20160102.
16 I. F. Ertis and I. Boz, *Mod. Res. Catal.*, 2017, **06**, 1–14.
17 X. Chen and C. Burda, *J. Am. Chem. Soc.*, 2008, **130**, 5018–5019.
18 X. Chen, L. Liu and F. Huang, *Chem. Soc. Rev.*, 2015, **44**, 1861–1885.
19 M. J. Sampaio, R. R. Bacsa, A. Benyounes, R. Axet, P. Serp, C. G. Silva, A. M. T. Silva and J. L. Faria, *J. Catal.*, 2015, **331**, 172–180.

20 J.-X. Jiang, F. Su, C. D. Wood, N. L. Campbell, H. Niu, C. Dickinson, A. Y. Ganin, M. J. Rosseinsky, Y. Z. Khimyak, A. I. Cooper and A. Trewin, *Angew. Chem., Int. Ed.*, 2007, **46**, 8574–8578.
21 Y. Xu, S. Jin, H. Xu, A. Nagai and D. Jiang, *Chem. Soc. Rev.*, 2013, **42**, 8012–8031.
22 A. G. Slater and A. I. Cooper, *Science*, 2015, **348**, aaa8075.
23 K. Zhang, D. Kopetzki, P. H. Seeberger, M. Antonietti and F. Vilela, *Angew. Chem., Int. Ed.*, 2013, **52**, 1432–1436.
24 R. S. Sprick, J. X. Jiang, B. Bonillo, S. Ren, T. Ratvijitvech, P. Guiglion, M. A. Zwijnenburg, D. J. Adams and A. I. Cooper, *J. Am. Chem. Soc.*, 2015, **137**, 3265–3270.
25 L. Cai, Y. Li, Y. Li, H. Wang, Y. Yu, Y. Liu and Q. Duan, *J. Hazard. Mater.*, 2018, **348**, 47–55.
26 B. Wang, Z. Xie, Y. Li, Z. Yang and L. Chen, *Macromolecules*, 2018, **51**, 3443–3449.
27 M. Bednarz, J. Lapin, R. McGillicuddy, K. M. Pelzer, G. S. Engel and G. B. Griffin, *J. Phys. Chem. C*, 2017, **121**, 5467–5479.
28 Z. Guan, H.-W. Li, Y. Cheng, Y. Zhao, M.-F. Lo, S.-W. Tsang and C.-S. Lee, *ACS Appl. Mater. Interfaces*, 2018, **10**, 7256–7262.
29 H.-J. Hou, X.-H. Zhang, D.-K. Huang, X. Ding, S.-Y. Wang, X.-L. Yang, S.-Q. Li, Y.-G. Xiang and H. Chen, *Appl. Catal., B*, 2017, **203**, 563–571.
30 S. Ren, R. Dawson, A. Laybourn, J.-x. Jiang, Y. Khimyak, D. J. Adams and A. I. Cooper, *Polym. Chem.*, 2012, **3**, 928–934.
31 Y. W. Li, Q. Duan, H. G. Wang, B. Gao, N. N. Qiu and Y. H. Li, *J. Photochem. Photobiol., A*, 2018, **356**, 370–378.
32 Z. Xiao, Y. Zhou, X. Xin, Q. Zhang, L. Zhang, R. Wang and D. Sun, *Macromol. Chem. Phys.*, 2016, **217**, 599–604.
33 H. Zhang, R.-L. Zong, J.-C. Zhao and Y.-F. Zhu, *Environ. Sci. Technol.*, 2008, **42**, 3803–3807.
34 Y. Xiang, X. Wang, X. Zhang, H. Hou, K. Dai, Q. Huang and H. Chen, *J. Mater. Chem. A*, 2018, **6**, 153–159.